Glycoconjugate Journal 15, 1001–1016 (1998)

Two novel isoneolacto-undecaglycosylceramides carrying Galα1→3Lewis^x on the 6-linked antenna and *N*-acetylneuraminic acidα2→3 or Galactose α1→3 on the 3-linked antenna, expressed in porcine kidney

Danièle Bouhours[1]*, Jérôme Liaigre[1,2], Jérôme Lemoine[3], Franz Mayer-Posner[4] and Jean-François Bouhours[1]

[1]*Institut de Transplantation et de Recherche en Transplantation, INSERM U.437, Centre Hospitalier Universitaire, F-44093 Nantes Cedex 1, France*
[2]*Laboratoire de Synthèse Organique, CNRS-UMR6513, Faculté des Sciences et des Techniques de Nantes, F-44072 Nantes, France*
[3]*CNRS-UMR111, Université des Sciences et Techniques, Villeneuve d'Ascq, France*
[4]*Bruker-Franzen Analytik, Bremen, Germany*

Three sialosylated and three neutral glycosphingolipids sharing a common *iso*-neolacto core were isolated from porcine kidney cortex. They were purified by preparative HPTLC, and were characterized by partial exoglycosidase hydrolysis followed by thin layer chromatography and immunostaining with anti-Galα1→3Gal, anti-type 2 lactosamine and anti-Lewis^x antibodies, methylation analysis, MALDI-TOF mass spectrometry and ^{1}H-NMR spectroscopy. Among neutral glycolipids, one was a known structure, VI^{3}VI′^{3}(αGal)$_2$-*iso*-nLc$_8$Cer, and two were novel structures differing by the number of Galα3Lewis^x determinants: VI^{3}VI′^{3}(αGal)$_2$V′^{3}αFuc-*iso*-nLc$_8$, and VI^{3}VI′^{3}(αGal)$_2$ V^{3}V′^{3}(αFuc)$_2$-*iso*-nLc$_8$. The single Galα3Lewis ^{x} determinant was found on the 6-linked antenna. Among sialosylated glycolipids, two had been previously found in other species and tissues, VI^{3}VI′^{3}(NeuAc)$_2$-*iso*-nLc$_8$, and VI^{3}NeuAcVI′^{3}αGal-*iso*-nLc$_8$. A novel structure was discovered presenting a Galα3Lewis^x determinant on the 6-linked antenna and a *N*-acetylneuraminic acid on the 3-linked antenna, VI^{3}NeuAcVI′^{3}αGalV′^{3}αFuc-*iso*-nLc$_8$. These results indicate that, *in vivo,* the porcine kidney α3fucosyltransferase synthesizes the Galα3Lewis^x determinant, acting on the 6-linked before the 3-linked Galα3neolactosamine, and appears unable to synthesize the sialosylated Lewis^x determinant on neolactoseries glycolipids.

Keywords: **glycoshingolipids, kidney, Lewis^x, nuclear magnetic resonance, mass spectrometry, pig, xenotransplantation, fucosyltransferase** ***Abbreviations:*** **HPTLC, high performance thin layer chromatography; MALDI-TOF MS, matrix-assisted laser desorption/ionization time of flight mass spectrometry; Me$_2$SO-*d*$_6$, hexadeuterated dimethyl sulfoxide; *SGL, Sialosylated glycolipids*.**

Introduction

Interest in the characterization of swine antigens recognized by human natural antibodies has been stimulated by the emergence of xenotransplantation of porcine organs as a possible mean to alleviate the shortage of human organ donors. The major barrier to xenotransplantation consists of natural antibodies present in human serum [1], which are essentially reactive with the disaccharide determinant Galα1→3Gal present at the nonreducing end of the oligosaccharide chains of glycoproteins and glycolipids of the animal donor [2–4]. The human species develops such antibodies because it does not express the epitope, like Old World monkeys and birds, in contrast with all the other species which are Galα1→3Gal-expressing [5, 6]. Lack of expression in human is linked to inactivation of the afucoB α3-galactosyltransferase gene in the Hominid lineage 20 million years ago [6, 7].

*To whom correspondence should be addressed.

Lactoseries glycosphingolipids terminated by Galα1→3Gal (afucoB epitope) (Table 1) were first described in rabbit [8–10] and bovine [11, 12] erythrocytes. Characterization of Galα1→3Gal-terminated glycosphingolipids in porcine organs likely to be transplanted, such as kidney, has been undertaken as a first step to elucidate the molecular specificity of natural human anti-Galα1→3Gal antibodies. At the begining of our study, it was known that IV^{3}αGal-nLc$_4$Cer (afucoB-5, Table 1) was expressed in porcine kidney [13, 14]. We have discovered and characterized a series of novel neutral glycolipids in which the Galα1-3Gal disaccharide is presented as Galα1→3Le^x determinant (GLe^x): IV^{3}αGalIII^{3}αFuc-nLc$_4$Cer (GLe^x-6), VI^{3}αGalV^{3}αFuc-nLc$_6$Cer (GLe^x-8) and VI^{3}VI′^{3}(αGal)$_2$V^{3}V′^{3}(αFuc)$_2$-*iso*-nLc$_8$Cer (GLe^x-12) [15]. In this first study, GLe^x-12 was copurified with a GL-11, which appeared as a glycolipid presenting both the afucoB and the GLe^x determinants. Complete characterization of GL-11 as VI^{3}VI′^{3}(αGal)$_2$V′^{3}αFuc-*iso*-nLc$_8$Cer was carried out in the present work. In parallel, it was also demonstrated that afucoB-10 (GL-10), VI^{3}VI′^{3}(αGal)$_2$-*iso*-nLc$_8$Cer, previously characterized in rabbit erythrocytes [10], was a component of pig kidney cortex. Existence of the hybrid structure GL-11 and structural analogy of the GLe^x determinant with the human sialosylated Le^x determinant (SLe^x) prompted us to investigate the sialosylated glycolipids of porcine kidney cortex. Three *iso*-nLc$_8$ core sialosylated glycolipids were characterized. Two were similar to already described glycolipids: VI^{3}VI′^{3}(αNeuAc)$_2$-*iso*-nLc$_8$Cer of human type O erythrocytes [16], and VI^{3}αNeuGcVI′^{3}αGal-*iso*-nLc$_8$Cer of bovine erythrocytes [11, 12]. The third one was a novel structure, VI^{3}αNeuAcVI′^{3}αGalV′^{3}αFuc-*iso*-nLc$_8$Cer (SM1), that presented the GLe^x determinant in addition to the sialosyl residue which was not expressed as SLe^x.

Materials and methods

Purification of glycosphingolipids

Porcine kidneys were collected at a local slaughterhouse. The cortex was dissected, minced, and lyophilized. Lipids were extracted from fractions of 5 g of lyophilized cortex of individual swine, as already described [17]. Glycolipids were purified by chromatography of the acetylated lipid extract on a Florisil column [18] (3 g Florisil per g lyophilized tissue) successively eluted with 1- 2-dicholoroethane (10 ml per g Florisil), 1-2-dichloroethane/acetone (93:7) (10 ml per g Florisil), and 1-2-dichloroethane/acetone (1:1) (20 ml per g Florisil). The glycolipid fraction eluted in the last step was deacetylated and desalted by dialysis before separation of neutral and sialosylated glycolipids on a column of DEAE-Sephadex A-25, acetate form [19]. Either total sialosylated glycolipids were recovered by elution with 0.5 M Na acetate in methanol, or a two-step elution was used to separate monosialosylated glycolipids (0.05 M Na acetate in methanol) and polysialosylated glycolipids and sulfatide (0.5 M Na acetate in methanol). Glycolipids were chromatographed on Silica Gel 60 HPTLC glass plates (Merck, Chelles, France) developed in chloroform/methanol/water, 50: 40:10 containing 0.25% $CaCl_2$ for sialosylated glycolipids (solvent A), and 60:35:8 for neutral glycolipids (solvent B), and visualized by their fluorescence in UV light after spraying a 0.01% solution of primulin in acetone/water (8:2). Glycosphingolipids were purified by repetitive preparative HPTLC, scraping of the fluorescent glycolipid bands, and extraction from the gel in chloroform/methanol/water (30:60:8). Primulin was removed from neutral glycolipids by DEAE Sephadex A-25 (acetate form) column chromatography [15].

Quantitative measurement

Quantities of glycolipids were determined by measurement of sphingosine content, according to a procedure described earlier [20].

Degradation by exoglycosidases

Cleavage of terminal sialic acid was obtained by incubation of an aliquot of 5 nmol of sialosylated glycolipid with 100 mU of *V. cholerae* neuraminidase (Behring, Rueil-Malmaison, France). Cleavage of terminal α -Gal was obtained by incubation of an aliquot of 5-10 nmol of glycolipid with 50 mU of α-galactosidase from green coffee beans (Boehringer) in 50 mM citrate buffer at pH 4. After incubation overnight at 37°C, samples were desalted by reverse phase chromatography on a Sep-Pak $C_1$8 cartridge. In case of successive hydrolysis by both enzymes, samples were chromatographed on Sep-Pak after each hydrolysis. Hydrolyzed glycolipids were identified by TLC-immunostaining with the proper antibodies. Free sialic acids obtained after hydrolysis with *V. cholerae* neuraminidase were purified by chromatography on Dowex 50W-X8 resin as described earlier [21] and analyzed by HPTLC in 1-propanol/2.5 M aqueous ammonia (7:3).

HTLC-immunostaining

Glycolipids were chromatographed on Silica Gel 60 HPTLC aluminum-backed plates developed in solvent A (sialosylated glycolipids) or solvent B (neutral and desialosylated glycolipids). Chromatograms were immunostained as already described [22] with anti-A (NaM87-1F6, Centre Régional de Transfusion Sanguine, Nantes, France), anti-Le^a (7-LE) (kindly supplied by Dr. J LePendu), anti-Le^x (CD15) (8-OH5, Immunotech, Marseille, France), and anti-type 2 lactosamine (1B2) [23] murine monoclonal antibodies, and anti-Galα1→3Gal chicken polyclonal antibodies affinity-purified on Synsorb Galα1→3Gal (Chembiomed) [24]. Mouse monoclonal antibodies were detected by reac-

Table 1. Glycolipid structures

Glycolipid nomenclature	*Abbreviated carbohydrate nomenclature*	*Name*
IV^{3}αGal-nLc$_4$Cer	Galβ4GlcNAcβ3Galβ4GlcβCer / Galα3	afucoB-5
IV^{3}αGal III^{3}αFuc-nLc$_4$Cer	Galβ4GlcNAcβ3Galβ4GlcβCer / \ Galα3 Fucα3	GLe^x-6
VI^{3}VI'^{3}(αGal)$_2$-*iso*-nLc$_8$Cer	Galα3 \ Galβ4GlcNAcβ6 \ Galβ4GlcNAcβ3Galβ4GlcβCer / Galβ4GlcNAcβ3 / Galα3	afuco-B10
VI^{3}VI'^{3}(αGal)$_2$V^{3}V'^{3}(αFuc)$_2$-*iso*-nLc$_8$Cer	Galα3 Fucα3 \ \ Galβ4GlcNAcβ6 \ Galβ4GlcNAcβ3Galβ4GlcβCer Galβ4GlcNAcβ3 / \ Galα3 Fucα3	GLe^x-12
VI^{3}VI'^{3}(αGal)$_2$V'^{3}αFuc-*iso*-nLc$_8$Cer	Galα3 Fucα3 \ \ Galβ4GlcNAcβ6 \ Galβ4GlcNAcβ3Galβ4GlcβCer / Galβ4GlcNAcβ3 / Galα3	GLe^x-11
VI^{3}VI'^{3}(NeuAc)$_2$-*iso*-nLc$_8$Cer	NeuAcα3 \ Galβ4GlcNAcβ6 \ Galβ4GlcNAcβ3Galβ4GlcβCer / Galβ4GlcNAcβ3 / NeuAcα3	SD1
VI^{3}NeuAcVI'^{3}αGal-*iso*-nLc$_8$Cer	Galα3 \ Galβ4GlcNAcβ6 \ Galβ4GlcNAcβ3Galβ4GlcβCer / Galβ4GlcNAcβ3 / NeuAcα3	SM2
VI^{3}NeuAcVI'^{3}αGalV'^{3}αFuc-*iso*-nLc$_8$Cer	Galα3 Fucα3 \ \ Galβ4GlcNAcβ6 \ Galβ4GlcNAcβ3Galβ4GlcβCer / Galβ4GlcNAcβ3 / NeuAcα3	SM1

tion with sheep biotinylated antimouse immunoglobulins (Amersham, 1:500 dilution), followed by labeling with streptavidin-horseradish peroxidase (HRP) conjugate. Chicken anti-Galα1→3Gal antibodies were detected with HRP-conjugated rabbit anti-chicken antibodies (Sigma Immunochemicals, 1:500 dilution). Visualization was obtained by chemiluminescence using the ECL-Western blotting kit (Amersham, Les Ulis, France) and short exposure to a blue-light sensitive autoradiography film (Hyperfilm ECL Western, Amersham).

Methylation analysis

Purified glycolipids were permethylated by the method of Ciucanu and Kerek [25]. The partially methylated glycolipids were submitted to acetolysis, reduction, and acetylation [26]. Gas chromatography of the partially methylated alditol acetates was done on a 25 m × 0.32 mm fused silica capillary column wall-coated with 0.2 μm of OV-1. Analyses were performed on a Hewlett Packard 5890 g as chromatograph equipped with a flame ionization detector and operated in constant flow mode. Carrier gas was helium at a velocity of 40 cm s^{-1}. Samples dissolved in hexane were injected (1 μl) on column at an oven temperature of 60°C. After 0.5 min, the oven temperature was raised to 125°C at a rate of 20°C min^{-1}, then up to 250°C at a rate of 5°C min^{-1}.

Matrix-assisted laser desorption/ionization time of flight (MALDI-TOF) mass spectrometry

MALDI mass spectra of permethylated glycolipids were recorded on a reflectron type Vision 2000 time-of-flight mass spectrometer (Finnigan, Bremen, Germany) in the positive ion mode. Samples were prepared by mixing on the target equal volumes of the glycolipid solution (typically 10–50 pmol in methanol) and a 12 mg/ml solution of 2,5-dihydroxybenzoic acid in methanol/water (70:30), and then allowed to dry at room temperature. Samples were mounted on a x,y movable stage allowing irradiation of selected samples and spot areas. A nitrogen laser with an emission wavelength of 337 nm and 3 ns pulse duration was used.

MALDI mass spectra of underivatized sialosylated glycolipids were acquired with a Bruker Reflex III MALDI-TOF mass spectrometer (Bruker-Franzen Analytik, Bremen, Germany). Samples were dissolved in methanol (10 pmol/μl) and mixed with a 15 mg/ml solution of 2,5-dihydroxybenzoic acid in methanol. The mixture was dried on a stainless steel sample holder and introduced into the ion source. Positive ions were recorded in the reflectron mode and Pulsed Ion Extraction was applied.

^{1}H NMR spectroscopy

Native glycolipids were equilibrated three times in deuterated methanol and dried under nitrogen. They were dissolved in 0.5 ml of Me_2SO-d_6/2% D_2O. Spectra were recorded at 400 MHz with 0.4 Hz digital resolution on a Bruker ARX-400 spectrometer. The probe temperature was 55°C. Chemical shifts are given relative to tetramethylsilane.

Results

Swine has an A/H genetic polymorphism [27], which is similar to human blood group A/B/H polymorphism without B expression. The porcine A and H determinants are histo groups. Kidney of commonly available swines expresses either A- and H-active glycolipids, or only H-active glycolipids [28]. As for the characterization of Galα1→3Le^x hexaglycosylceramide in porcine kidney [15], the present investigation that was aimed at studying complex Galα1→3Gal terminated glycolipids was carried out with material from non-A porcine kidney only, in order not to be hampered by A-active glycolipids, which often co-migrate with Galα1→3Gal terminated glycolipids. For that purpose, glycolipids were purified from kidney cortex of individual animals and tested for the expression of A-active glycolipids by HPTLC-immunostaining of neutral and sialosylated glycolipids with a monoclonal anti-A antibody. It is worth noticing that A-active glycolipids were only found in neutral glycolipids. Glycolipids samples from non-A kidneys were further processed for structural analysis of complex glycolipids.

HPTLC, methylation analysis, and mass spectrometry of neutral glycolipids

In our previous study characterizing Galα1→3Le^x hexaglycosylceramide (GLe^x-6), it was observed that the most polar band of the chromatogram of neutral glycolipids actually contained two glycolipids, termed GL-11 and GL-12 (Table 1), which yielded a nona- and a decaglycosylceramides on α-galactosidase hydrolysis, both reactive with anti-Le^x mAb [15]. The presence of Lewis-type structures was confirmed by methylation analysis, as the chromatogram of partially methylated alditol acetates displayed peaks of 2,3,4-tri-*O*-Me-Fuc (Fuc1→) and 6-*O*-Me-GlcNAcMe (→3,4GlcNAc1→) [15].

In the present study, three very faint fluorescent bands were visualized under UV light after primulin spraying almost at the origin of the chromatogram of neutral glycolipids of kidney of 2-year-old pigs (Figure 1, Panel A, K0, K1, and K2). They accounted for 0.5% of neutral glycolipids (50 nmol per kidney). The three chromatographic bands were tentatively isolated. Purified fractions K0, K1, and K2 were reactive with anti-Galα1→3Gal antibodies (Figure 1, Panel B). HPTLC-immunostaining after α-galactosidase hydrolysis indicated that K0 and K1 were heterogeneous. Both degalactosylated glycolipid fractions contained two glycolipids reactive with CD15, the less po-

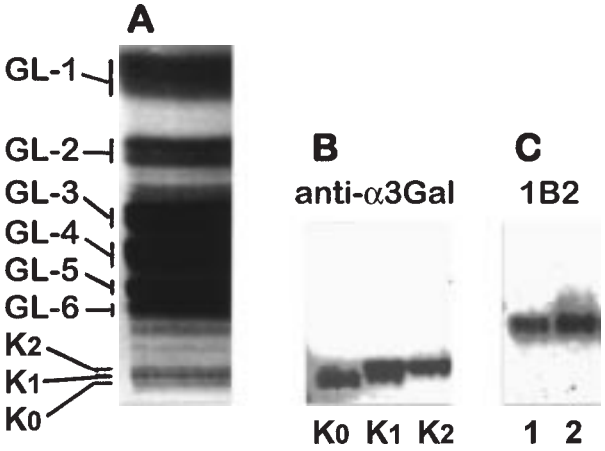

Figure 1. HPTLC of neutral glycosphingolipids of porcine kidney. Panel A, visualization with UV light after spraying with primulin (0.01% in acetone/water, 8:2). Panel B, immunostaining of purified fractions K0, K1 and K2 with chicken anti-Galα1→3Gal antibodies. Panel C, immunostaining with 1B2 of K2 after hydrolysis with α-galactosidase (lane 1) and H_3 ($VI^3VI'^3(\alpha Fuc)_2$-*iso*-nLc_8Cer) from human blood group O erythrocytes [29] after hydrolysis with α-L-fucosidase (lane 2). Chromatograms were developed in chloroform/methanol/water (60:35:8). GL-1, monohexosylceramide; GL-2, lactosylceramide; GL-3, Gb_3Cer; GL-4, Gb_4Cer; GL-5, $IV^3\alpha Gal$-nLc_4Cer; GL-6, $IV^3\alpha Gal\ III^3\alpha Fuc$-$nLc_4Cer$.

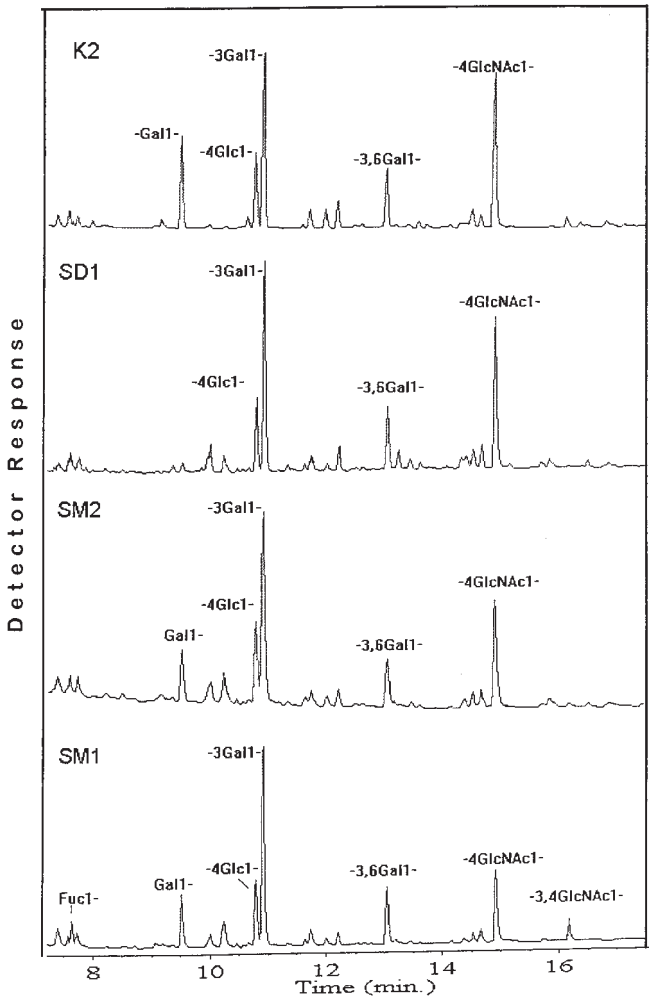

Figure 2. Gas chromatography of the partially methylated alditol acetates of Galα1→3Gal-terminated neutral glycolipid K2/GL-10, and sialosylated glycolipids SM1, SM2 and SD1.

lar being in addition reactive with 1B2 (not shown), as in our previous work [15]. Native and degalactosylated K0 and K1 were not reactive with anti-Le^a mAb (not shown).

K2 was purified to near homogeneity from kidney of 3-month-old pigs, previously shown to express less Gle^x determinants than kidney of older pigs [15]. The glycolipid resulting from α-galactosidase hydrolysis of K2, but not native K2, was reactive with 1B2 (Figure 1, panel C-lane 1). It had the same chromatographic mobility as the *iso*-nLc_8Cer obtained after defucosylation of the neutral glycolipid H_3 from human blood group O erythrocytes ($VI^3VI'^3(\alpha Fuc)_2$-*iso*-nLc_8Cer) [29] (Figure 1, Panel C-lane 2). The GC profile of the partially methylated alditol acetates of K2 (Figure 2) displayed peaks for 2,3,4,6-tetra-*O*-Me-Gal (Gal1→), 2,3,6-tri-*O*-Me-Glc (→4Glc1→), 2,4,6-tri-*O*-Me-Gal (→3 Gal1→), 2,4-di-*O*-Me-Gal (→3,6Gal1→), and 3,6-di-*O*-Me-GlcNAcMe (→4Glc NAc1→), which were consistent with type 2 chain and branching GlcNAc1→3 and GlcNAc1→6 to Gal. HPTLC-immunostaining and methylation analysis indicated that the K2 fraction contained a Galα1→3Gal-terminated GL-10 with an *iso*-nLc_8 core (Table 1). This conclusion was supported by the MALDI-TOF mass spectrum of permethylated K2 (Figure 3, Panel A), which was composed of five major peaks corresponding to pseudomolecular ions $(M + Na)^+$ for $Hex_7HexNAc_3$ plus ceramide with fatty acids with 16 (*m/z* 2769) to 24 carbon atoms (*m/z* 2 881) (GL-10).

The MALDI-TOF mass spectrum of permethylated K1 (Figure 3, Panel B) displayed major peaks for pseudomolecular ions $(M + Na)^+$ for $Hex_7HexNAc_3Fuc_1$ (GL-11) plus ceramide with fatty acids with 16 (*m/z* 2943) to 24 (*m/z* 3055) carbon atoms. Two groups of peaks of lesser intensity were also observed. One group corresponded to $(M + Na)^+$ ions for GL-10 with ceramide with C16, C18, and C20 fatty acids (*m/z* 2769, 2797, 2825), the major peak being for C16 fatty acid. The second additional group of peaks (*m/z* 3117 to 3229) corresponded to $(M + Na)^+$ ions for $Hex_7HexNAc_3Fuc_2$ plus ceramide with predominantly C20, C22, and C24 fatty acids (*m/z* 3173, 3201, 3229, respectively). In conclusion, K1 contained GL-11 together with GL-10 with shorter chain fatty acids and GL-12 with longer chain fatty acids. The pseudomolecular ions evidenced a difference of 174 mass units between homologous structures, demonstrating that GL-11 and GL-12 differed from GL-10 by addition of one and two fucose residues, respectively.

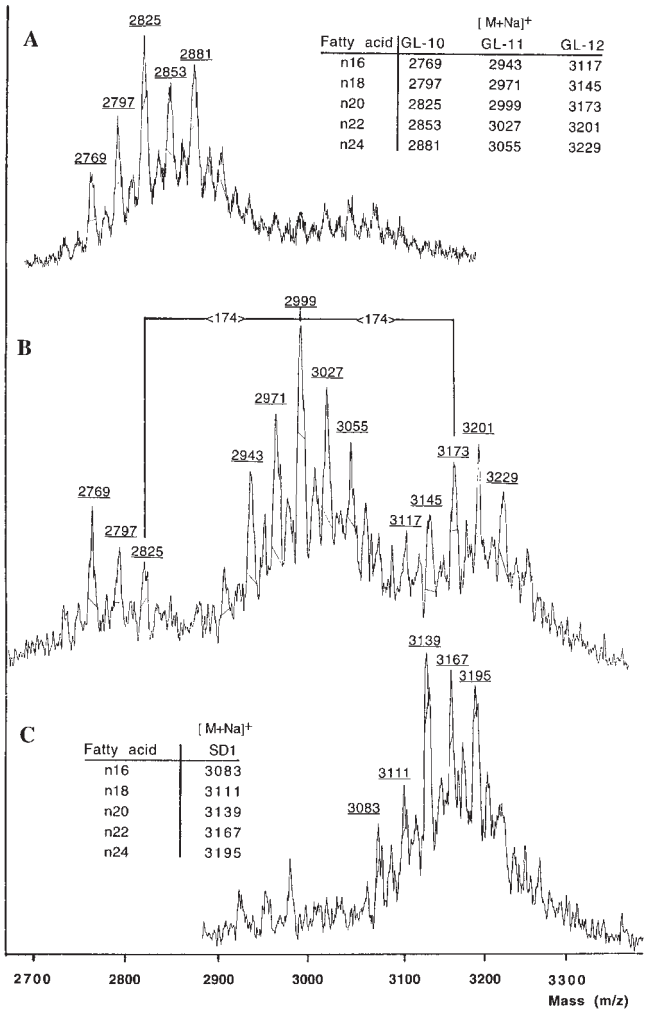

Figure. 3. MALDI-TOF mass spectra in the positive ion mode of the permethylated neutral glycosphingolipid fractions K1 and K2, and sialosylated SD1. Panel A, spectrum of permethylated K2 corresponding to GL-10. Panel B, spectrum of permethylated K1 containing GL-10, GL-11 and GL-12, demonstrating that the three structures differ from each other by 174 mass units (one fucose residue). Panel C, spectrum of permethylated sialosylated SD1.

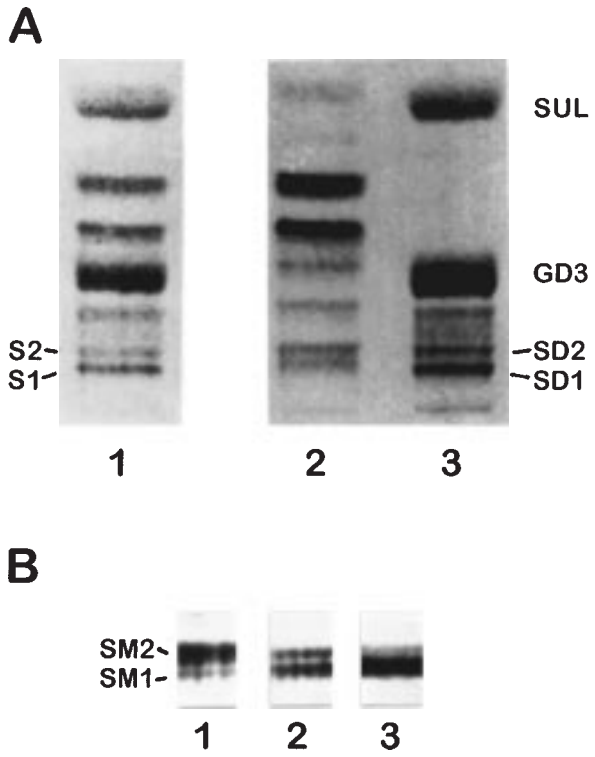

Figure 4. HPTLC of sialosylated glycosphingolipids of porcine kidney. Panel A, lane 1, total sialosylated glycolipids; lane 2, monosialosylated glycolipids; lane 3, polysialosylated glycolipids and sulfatide. Panel B, monosialosylated glycolipids SM1 and SM2 at different ages corresponding to different kidney weights, 190 g (lane 1), 250 g (lane 2), and 390 g (lane 3). Chromatograms were developed in chloroform/methanol/water containing 0.25% $CaCl_2$ (50:40:10). Visualization with UV light after spraying with primulin (0.01% in acetone/water, 8:2). SUL, sulfatide; SPG, IV^3NeuAc-nLc_4Cer.

HPTLC, methylation analysis, and mass spectrometry of sialosylated glycolipids

Two slow migrating bands, which were called S1 and S2, were observed on visualization of the chromatogram of total sialosylated glycolipids (SGL) under UV light (Fig. 4, panel A-lane 1). They accounted for 8% of sialosylated glycolipids (400 nmol per kidney). After separation of mono- and poly-SGL, it appeared that S1 yielded a mono-SGL SM1 (Figure 4, Panel A-lane 2) and a poly-SGL SD1 (Figure 4, Panel A-lane 3). S2 also yielded a mono-SGL SM2 and a poly-SGL SD2. Repetitive HPTLC purifications of individual SGL were carried out. On HPTLC-immunostaining of concentrated purified mono- and poly-SGL, it appeared that only SM1 and SM2 reacted with anti-Galα1→3Gal antibodies (Figure 5, Panel A). The present work was focused on the structural characterization of SD1 and of Galα1→3Gal-terminated SM1 and SM2. SD2 is not described in the present study.

HPTLC-immunostaining after exoglycosidase hydrolysis gave some insight into the glycolipid structures. None of the native SGL reacted with anti-type 2 lactosamine 1B2, and anti-Le^x (CD15). *N*-acetylneuraminic acid was the only sialic acid released by neuraminidase hydrolysis of the total S1-S2 fraction. Hydrolysis of purified SM1, SM2, and SD1 with *V. cholerae* neuraminidase induced a change in their immunostaining reactivity (Figure 5, Panels B-C). This result indicated that α-NeuAc was linked to terminal glycosidic residues of all three glycolipids.

The glycolipid obtained after *V. cholerae* neuraminidase hydrolysis of SD1 strongly reacted with 1B2 (Figure 5, lane 3). Its chromatographic behavior identical with that of defucosylated H_3 (Figure 5, lane 4) suggested that SD1 also had an *iso*-nLc_8 core. This hypothesis was further supported by the GC profile of the partially methylated alditol acetates of SD1, which was identical with that of K2, without

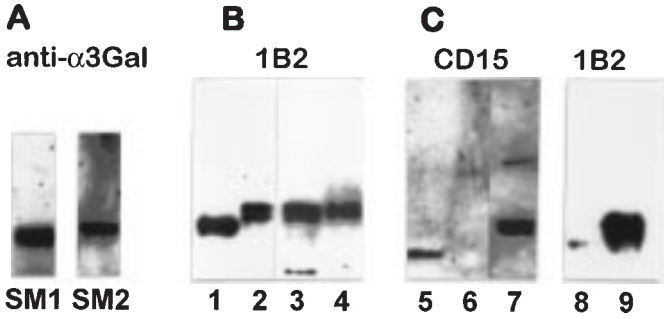

Figure 5. HPTLC and immunostaining of sialosylated glycosphingolipids. Panel A, immunostaining with chicken anti-Galα1→3Gal antibodies of SM1 and SM2 chromatographed in solvent A. Panel B, immunostaining with mAb 1B2 after HPTLC in solvent B of glycolipids obtained by hydrolysis of SM2 with *V. cholerae* neuraminidase (lane 1) and with both *V. cholerae* neuraminidase and α-galactosidase (lane 2), after hydrolysis of SD1 with *V. cholerae* neuraminidase (lane 3), and of H_3 with α-L-fucosidase (lane 4). Panel C, immunostaining with CD15 after HPTLC in solvent B of glycolipids resulting from SM1 hydrolysis with α-galactosidase (lane 5), *V. cholerae* neuraminidase (lane 6), and both *V. cholerae* neuraminidase and α-galactosidase (lane 7), and immunostaining with 1B2 after SM1 hydrolysis with *V. cholerae* neuraminidase (lane 8) and both *V. cholerae* neuraminidase and α-galactosidase (lane 9). Solvent A, chloroform/methanol/water 50:40:10 containing 0.25% $CaCl_2$; solvent B, chloroform/methanol/water 60:35:8.

peak for 2,3,4,6-tetra-*O*-Me-Gal (Gal1→) (Figure 2). Lack of derivatives for nonreducing terminal residues indicated the end-capping of both branches by NeuAc. SD1 was analyzed by MALDI-TOF mass spectrometry after permethylation (Figure 3, Panel C). Major pseudomolecular ions $(M + Na)^+$ at *m/z* 3139 (C20 fatty acid), 3167 (C22 fatty acid), and 3195 (C24 fatty acid) were consistent with a $Hex_5HexNAc_3NeuAc_2$ oligosaccharide chain.

Hydrolysis of SM2 by both *V. cholerae* neuraminidase and α-galactosidase yielded a 1B2-reactive glycolipid (Figure 5, lane 2), migrating like desialosylated SD1 (Figure 5, lane 3) and defucosylated H_3 (Fig. 5, lane 4). Hydrolysis of SM2 with only *V. cholerae* neuraminidase yielded a 1B2 reactive glycolipid (Figure 5, lane 1), which migrated one carbohydrate residue slower than desialosylated and degalactosylated SM2 (Figure 5, lane 2), and was still reactive with anti-Galα1→3Gal antibodies (not shown). This result was in favor of an *iso*-nLc_8 core with α-NeuAc on one antenna and α-Gal on the other antenna, although degalactosylated (sialosylated) SM2 could not be immunostained with 1B2. Degalactosylated (sialosylated) SM1 was reactive with anti-Le^x mAb (Figure 5, lane 5). Desialosylated (α-galactosylated) SM1 was reactive with 1B2 (Figure 5, lane 8) and was not immunostained with CD15 (Figure 5, lane 6). Hydrolysis of SM1 with both α-galactosidase and α-neuraminidase yielded a glycolipid immunostained with CD15 (Figure 5, lane 7) and 1B2 (Figure 5, lane 9). This double reactivity was in favor of a branched type 2 chain with one antenna carrying GLe^x and the other antenna carrying α-NeuAc. The relative contribution of SM1 and SM2 to the sialosylated glycolipid composition of porcine kidney appears to be developmentally regulated (Figure 4, Panel B). In younger animals, SM2 was more expressed than SM1, and it was the opposite in older animals.

The GC profile of the partially methylated alditol acetates of SM1 (Figure 2) displayed peaks for an *iso*-nLc carbohydrate chain as SM2, plus a peak for 6-O-*Me*-GlcNAcMe (→3,4GlcNAc1→) and a peak for 2,3,4-tri-*O*-Me-Fuc, as in the GC profile of the GL-12 fraction in our previous work [15]. The intensity of the peaks for Fuc1→ and →3,4GlcNAc1→ was in favor of one Lewis-type determinant in SM1.

Native sialosylated glycolipids SM1 and SM2 were analyzed by MALDI-TOF mass spectrometry. In the positive ion mode, two series of ions, $(M + Na)^+$ and $(M-H + 2Na)^+$, were observed for each glycolipid (Figure 6). The spectrum of SM2 displayed major pseudomolecular $(M + Na)^+$ ions between *m/z* 2434 (C16 fatty acid) and 2546 (C24 fatty acid), which were consistent with a $Hex_6HexNAc_3NeuAc_1$ oligosaccharide chain. The major pseudomolecular $(M + Na)^+$ ions of SM1 corresponded to those of SM2 plus one fucose residue (*m/z* 146), consistent with a $Hex_6HexNAc_3NeuAc_1Fuc_1$ oligosaccharide chain with C20 (*m/z* 2636) to C24 (*m/z* 2692) fatty acids.

^{1}H-NMR spectroscopy of neutral and sialosylated glycolipids

^{1}H-NMR spectra were interpreted by referring to spectra of *iso*-nLc core glycosphingolipids available in the literature (Table 2), either terminated with Galα1→3 (10), or with NeuAcα2→3 [16, 30].

^{1}H-NMR spectroscopy of SD1: Identification of $VI^3VI'^3(NeuAc)_2$-iso-nLc_8Cer

The 400 MHz ^{1}H-NMR spectrum of SD1 (Figure 7, Table 2) compared well with the spectrum of $VI^3VI'^3(NeuAc)_2$-*iso*-nLc_8Cer obtained at 308° K by Levery et *al.* [16]. It displayed typical signals for a nLc_6 core with attachment of a Galβ1→4GlcNAcβ1→6 branch at β-Gal IV (Table 2). The *iso*-nLc branching structure was supported by β-GlcNAc NAc signals in the acetamido-methyl region at 1.824 ppm (III) and at 1.843 ppm (V and V′) (Figure 8). The structural reporter groups for NeuAcα2→3 linked to Galβ1→4 were found in the acetamido-methyl region (α-NeuAc H-3_{eq} doublet of doublets at 2.748 ppm, and α-NeuAc NAc methyl resonance at 1.886 ppm), and their intensities were in favor of two terminal α-NeuAc (Figure 8). Also in favor of two terminal α-NeuAc was the intense doublet of doublets signal for β-Gal H-3 at 3.997 ppm (Figure 7), consistent with the resonances of two β-Gal H-1 protons VI-1 and VI′-1 at 4.220 ppm. The spectrum of SD1 was acquired from the S1 fraction containing both SD1 and SM1 (Figure 4, Panel A-lane 1). Therefore, additional lower intensity signals (Figure 7, a, b, c, and d) were interpreted as resonances of

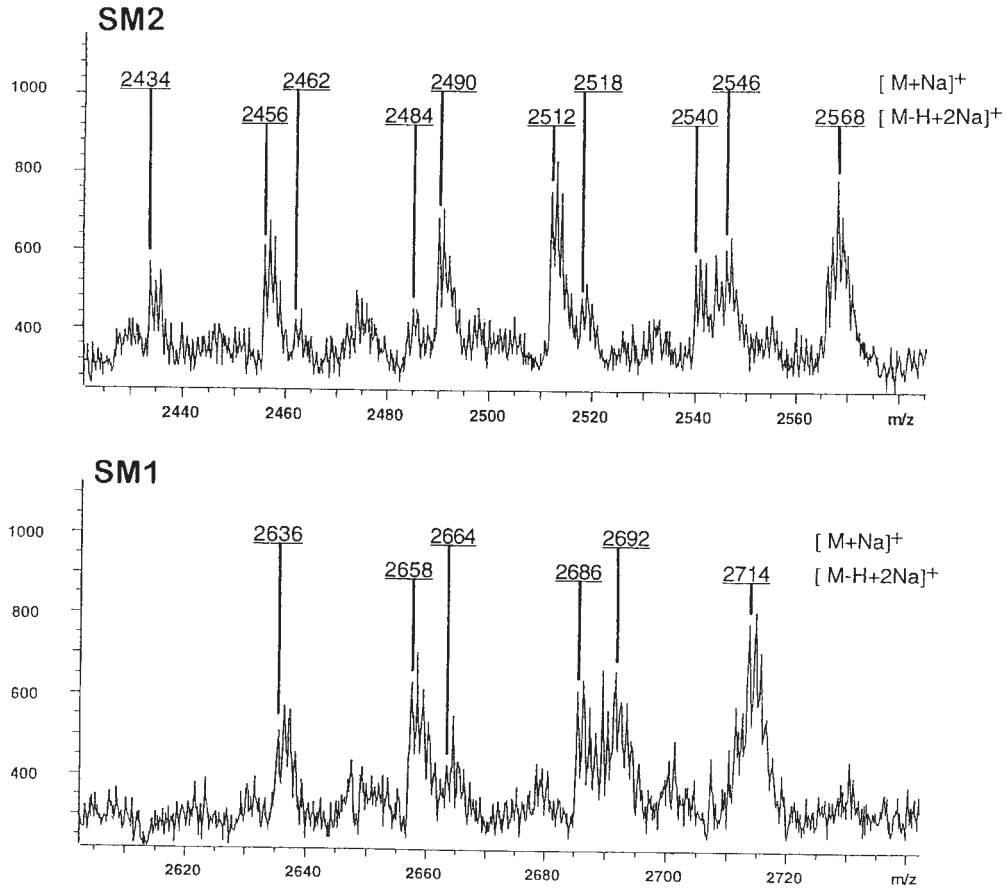

Figure 6. MALDI-TOF MS spectra of underivatized sialosylated *iso*-nLc$_8$ core glycolipids of porcine kidney cortex. SM1 and SM2 were analyzed as native glycolipids in the positive ion mode.

Galα1^{b}→3Galβ1^{d}→4(Fucα1^{a}→3)GlcNAcβ1^{c}→6 residues from SM1. The percentage contribution of SM1 to S1 was estimated at 25%. Such a small contamination did not impair the interpretation of the spectrum that fully supported the structure VI^{3}VI′^{3}(NeuAc)$_2$-*iso*-nLc$_8$Cer assigned to SD1.

^{1}H-NMR spectroscopy of K2: Identification of VI^{3}VI′^{3}(αGal)$_2$-iso-nLc$_8$Cer

The ^{1}H-NMR spectrum of K2 (Figure 9) displayed an intense α-anomeric proton signal at 4.850 ppm (Table 2), which was assigned to α-Gal (1→3) linked to a type 2 chain lactosamine [10, 13, 15]. The intensity of the signal, compared with the others, was consistent with the presence of two terminal α-Gal residues. The spectrum displayed eight β-anomeric H-1 signals compatible with an *iso*-n-Lc$_8$ core structure (Table 2). The *iso*-nLc branching structure was further supported by β-GlcNAc NAc signals at 1.826 ppm (III) and at 1.845 ppm (V and V′), compared with the singlet at 1.826 ppm observed for IV^{3}αGal-nLc$_4$Cer [15]. The intensity of the β-anomeric signal at 4.298 ppm was consistent with two similarly Galα1→3-substituted Galβ1→4 VI and VI′ (Figure 9). In conclusion, the ^{1}H-NMR spectrum of K2 could be assigned to the structure VI^{3}VI′^{3}(αGal)$_2$-*iso*-nLc$_8$Cer described by Hanfland et al. [10] in rabbit erythrocyte membranes.

^{1}H-NMR spectroscopy of SM2: Identification of VI^{3}NeuAcVI′^{3}αGal-iso-nLc$_8$Cer

The ^{1}H-NMR spectrum of SM2 (Figure 7) displayed an α-anomeric proton signal at 4.853 ppm which compared well with that of the K2 spectrum, and was thus assigned to terminal Galα1→3 (Table 2). The spectrum displayed eight β-anomeric proton signals compatible with an *iso*-nLc$_8$ core structure. The β-GlcNAc NAc signals further supporting the branching structure were observed at 1.826 and 1.848 ppm (III and V-V′, respectively) (Figure 8). The distinct resonances of VI-1 and VI′-1 were indicative of different terminal substituents. The presence of terminal NeuAcα2→3 in SM2 was manifested by the α-NeuAc NAc singlet at 1.887 p pm and the α-NeuAc H-3$_{eq}$ doublet of doublets at 2.751 ppm (Figure 8). The intensity of the signals, compared with that of the SD1 spectrum, were in favor of a single terminal α-NeuAc. The resonance of VI-1 at 4.220 ppm, as in SD1, was consistent with an α-NeuAc 1→3 linked to β-Gal VI, whereas the resonance of VI′-1 at 4.300 ppm, which compared well with that of K2, indicated

Table 2. Anomeric proton resonances for *iso*-nLc$_8$ core Glycosphingolipids.

VI′ V′
Galβ1-4GlcNAcβ1-6 IV III II I
\
Galβ1-4GlcNAcβ1-3Galβ1-4Glcβ1
/
Galβ1-4GlcNAcβ1-3
VI V

	α-Gal-VI-VI′	*α-Fuc-V-V′*	*VI′*	*V′*	*VI*	*V*	*IV*	*III*	*II*	*I*	*Ref*
VI^{3}NeuAc-*iso*-nLc$_8$			4.213	4.430	4.220	4.646	4.308	4.678	4.273	4.170	30
VI^{3}VI′^{3}(NeuAc)$_2$-*iso*-nLc$_8$			4.200	4.388	4.200	4.647	4.302	4.676	4.266	4.168	16[a]
VI^{3}VI′^{3}(NeuAc)$_2$-*iso*-nLc$_8$			4.220	4.416	4.220	4.681	4.319	4.705	4.288	4.172	this work SD1
VI^{3}NeuAcVI′^{3}αGal-*iso*-nLc$_8$	4.853		4.300	4.442	4.220	4.683	4.313	4.706	4.287	4.173	this work SM2
VI^{3}NeuAcVI′^{3}αGal V′^{3}αFuc-*iso*-nLc$_8$	4.850	4.893	4.358	4.516	4.223	4.686	4.318	4.706	4.289	4.173	this work SM1
III^{3}αFuc-nLc$_4$		4.876					4.295	4.748	4.280	4.206	31
IV^{3}αGal-nLc$_4$	4.83						4.32	4.72	4.29	4.16	13
IV^{3}αGal-nLc$_4$	4.847						4.316	4.705	4.286	4.170	15
IV^{3}αGalIII^{3}αFuc-nLc$_4$	4.843	4.889					4.354	4.785	4.286	4.169	15
VI^3,VI′^{3}(αGal)$_2$-*iso*-nLc$_8$	4.84		4.30	4.42	4.30	4.67	4.30	4.67	4.27	4.17	10
VI^{3}VI′^{3}(αGal)$_2$-*iso*-nLc$_8$	(4.850)$_2$		4.298	4.429	4.298	4.670	4.315	4.694	4.282	4.173	this work K2
VI′^{3}VI′^{3}(αGal)$_2$ V′^{3}αFuc-*iso*-nLc$_8$	(4.851)$_2$	4.886	4.351	4.525[b]	4.297	4.670	4.316	4.694	4.281	4.172	this work K1

[a]Acquired at 308K. Assignments for GlcNAc III-1 and V-1 given in ref. 16 are reversed in this table, as indicated in ref. 30
[b]Acquired from signal c in K2 (Fig. 7)

an α-Gal 1→3 linked to β-Gal VI′ (Table 2). The ^{1}H-NMR spectrum of SM2 was compatible with the structure VI^{3}NeuAcVI′^{3}αGal-*iso*-nLc$_8$Cer, in accordance with the reactivity with ant-Galα1- 3Gal antibodies (Figure 5, Panel A), with mAb 1B2 after *V. cholerae* neuraminidase and α-galactosidase hydrolysis (Figure 5, panel B, lanes 1–2), methylation analysis and MALDI-TOF mass spectrometry.

^{1}H-NMR Spectroscopy of SM1: Identification of VI^{3}NeuAcVI′^{3}αGalV′^{3}αFuc- iso-nLc$_8$Cer

The ^{1}H-NMR spectrum of SM1 (Figure 7) displayed two strong α-anomeric proton signals at 4.893 and 4.850 ppm (Table 2). The α-anomeric signal at 4.850 ppm fitted well the resonance observed for terminal α-Gal 1→3 linked to a lactosamine type 2 chain (Table 2). The α-anomeric signal at 4.893 ppm (Table 2) was consistent with the signal of an α-Fuc 1→3 linked to the β-GlcNAc residue of a Galα1→3 terminated type 2 chain described in IV^{3}αGalIII^{3}αFuc-nLc$_4$Cer [15]. The typical quartet at 4.624 ppm for the H-5 resonance (Figure 7, Table 3) and the doublet for the H-6 methyl group at 1.028 ppm (Figure 8; Table 3) were supporting signals for a Le^x-type Fucα1→3. It was also noticeable that, as observed by Levery et al. [16, 31], the chemical shift of the H-6 methyl proton resonance (1.028 ppm, Table 3) was in favor of a Fuc substituting the outer GlcNAc, as in IV^{3}αGal III^{3}αFuc-nLc$_4$ (1.031 ppm) [15], whereas for an inner substitution, it would have resonated upfield (1.014 ppm) [16, 30, 31]. The linkage of Fucα1→3 was assigned after analysis of the chemical shifts it induced in the core structure. Characteristic signals for an iso-nLc$_8$ core were observed in the anomeric region (Table 2). The βGlcNAc NAc signals at 1.825, 1.843, and 1.851 ppm (III, V, and V′, respectively) supported the branching structure (Figure 8). As in SM2, the terminal β-Gal VI and VI′ had distinct resonances, indicating different substituents. The presence of terminal NeuAcα2→3 was attested by the NeuAc NAc singlet at 1.888 ppm, the NeuAc H- 3$_{eq}$ doublet of doublets at 2.747 ppm (Figure 8), and the VI-3 doublet of doublets at 4.023 ppm (Figure 7). The VI-1 resonance at 4.223 ppm, as in SD1 and SM2, was consistent with the linkage of α-NeuAc to →3Galβ1→4GlcNAcβ1→3. The downfield shift of the V′-1 resonance, similar to that of SM1, indicated that α-Fuc was 1→3 linked to →4GlcNAcβ1→6. The downfield shift of β-Gal VI′-1 compared with that of K2 could be interpreted as the deshielding effect of the vicinal Le^x-

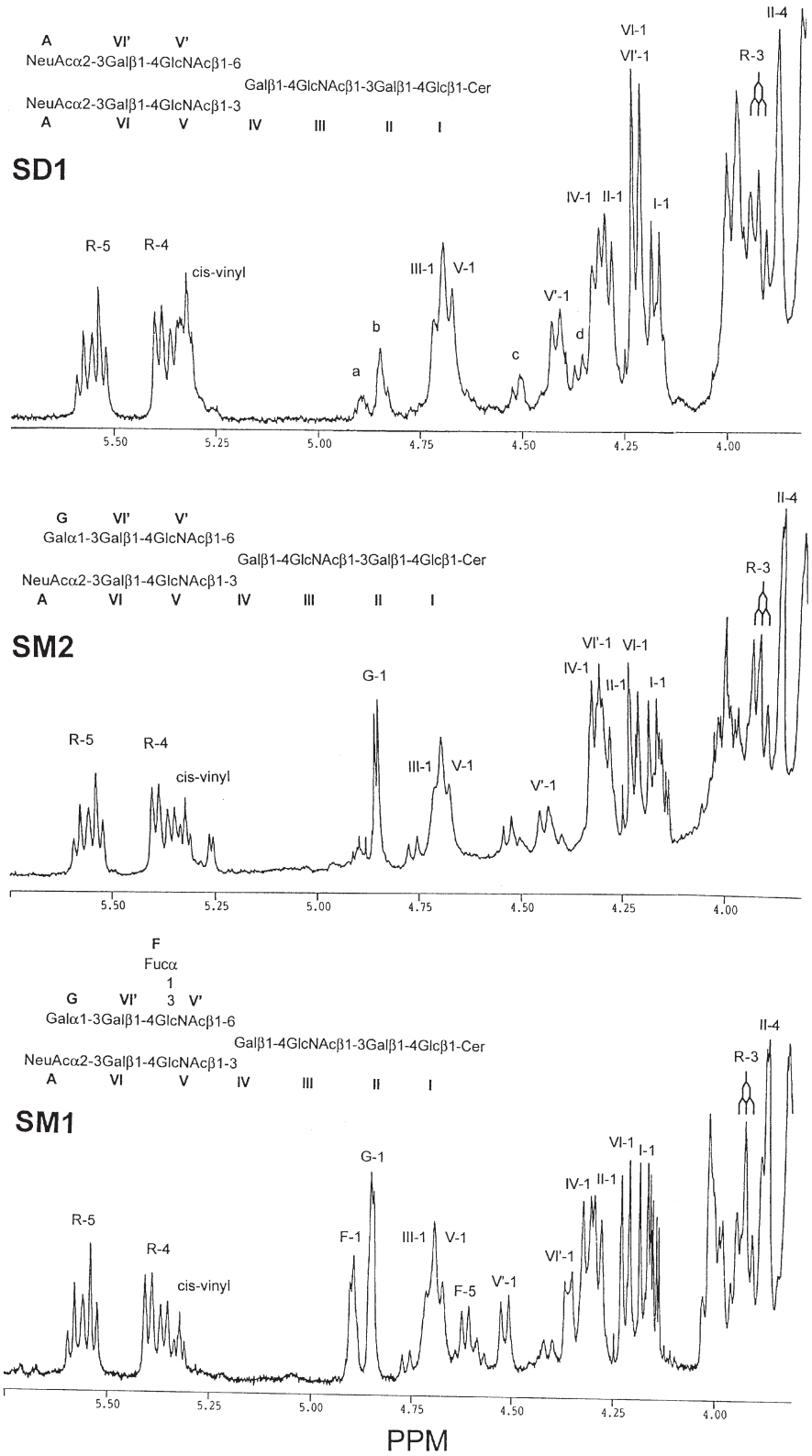

Figure 7. Downfield region of 400 MHz ^{1}H NMR spectra of sialosylated glycosphingolipids of pig kidney in Me_2SO-d_6/2%D_2O at 328° K. Arabic numerals refer to ring protons of residues designated by Roman numerals or capital letters. A refers to NeuAcα2→3, G to Galα1→3 and F to Fucα1→3. R refers to protons of the sphingosine core, cis-vinyl to protons adjacent to double bond of unsaturated fatty acids. Lower case letters in the SD1 spectrum indicate protons from the Galα1→3Le^x residues of contaminant SM1 (Table 2): a, α-Fuc; b, α-Gal; c, V′-1; d, VI′-1.

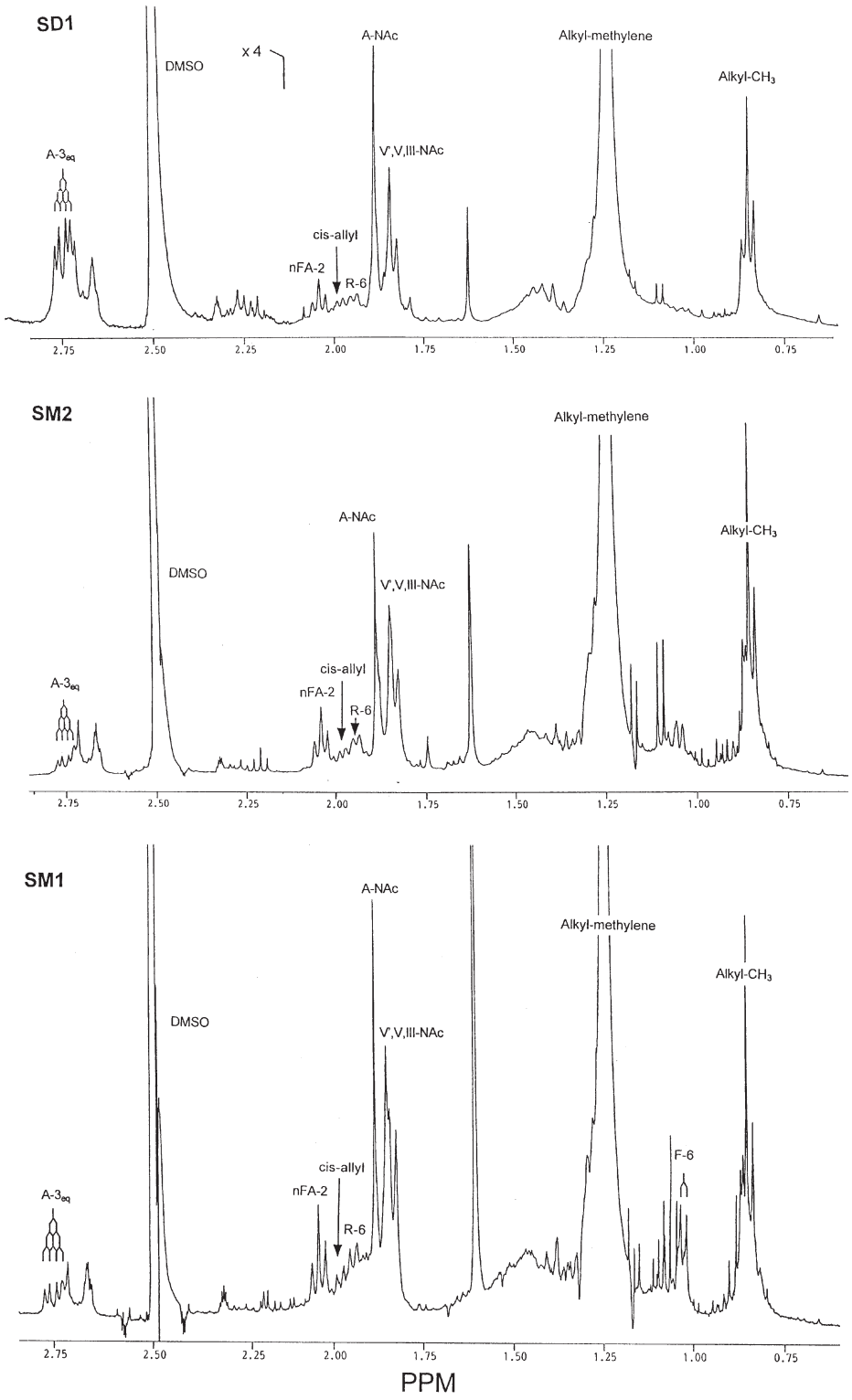

Figure 8. Upfield region of 400 MHz ^{1}H NMR spectra of sialosylated glycosphingolipids of pig kidney in Me_2SO-d_6/2%D_2O at 328° K.

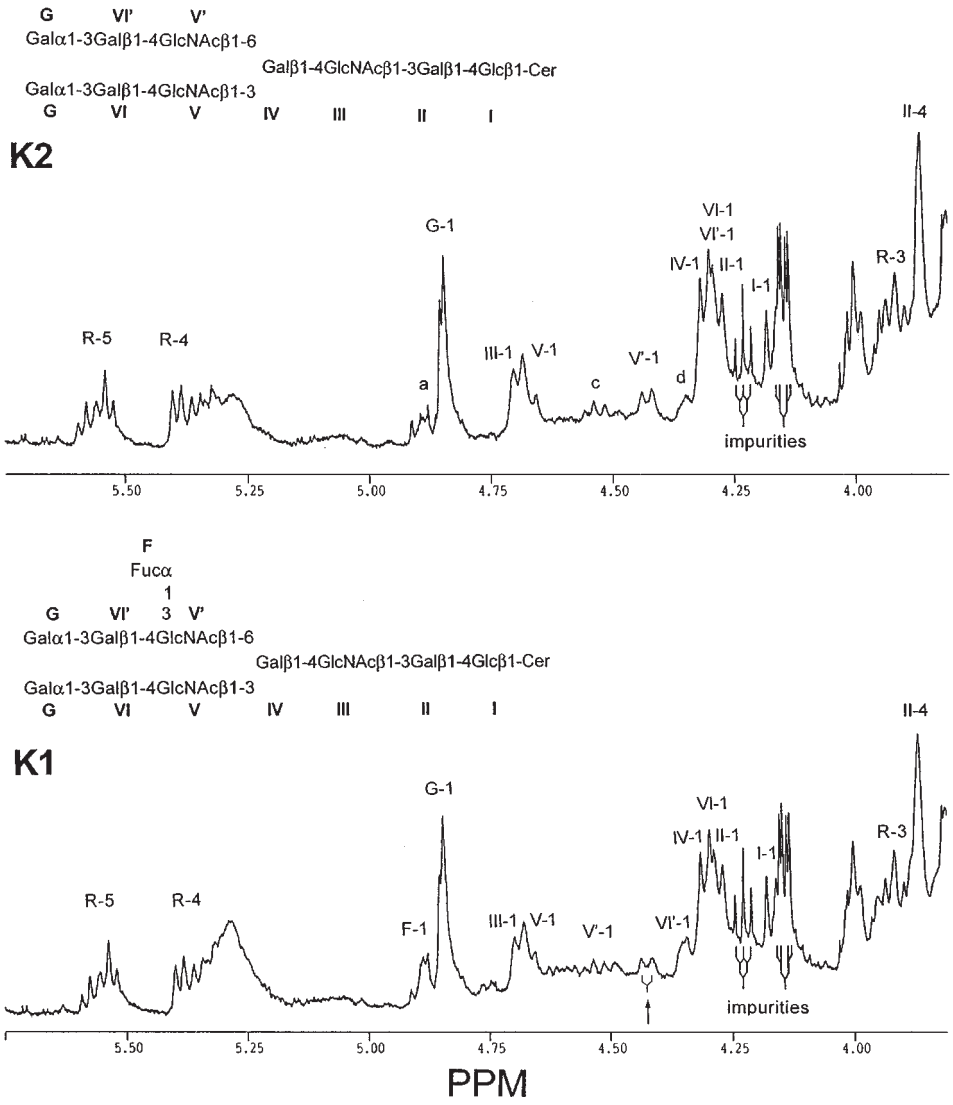

Figure 9. Downfield region of 400 MHz ^{1}H NMR spectra of neutral glycosphingolipids of pig kidney in Me_2SO-d_6/2% D_2O at 328° K. Lower case letters in the spectrum of K2 indicate protons from a small amount of K1 : a, α-Fuc-1; c, V′-1; d, VI′-1 (Table 2). Arrow in the K1 spectrum indicates V′-1 from K2 contaminant.

type Fucα1→3, as observed in IV^{3}αGal III^{3}αFuc-nLc$_4$ [15]. The VI′-1 resonance was consistent with Galα1→3 linkage to β-Gal VI′. The ^{1}H-NMR spectrum of SM1 was in favor of a novel structure composed of an α2→3 sialosylated nLc$_6$ core with a Galα1→3Le^{x}β1→6 branch at β-Gal IV. It was in agreement with the methylation (Figure 2) and MALDI-TOF (Figure 3) analyses, and with the reactivity of the native glycolipid with anti-Galα1→3Gal antibodies (Figure 5, Panel A). In addition, it fitted well the CD15 and 1B2 reactivities after α-galactosidase and *V. cholerae* neuraminidase hydrolysis (Figure 5, Panel C).

^{1}H-NMR Spectroscopy of K1: Identification of VI^{3}VI′3(αGal)$_2$V′^{3}αFuc-iso-nLc$_8$

As already indicated, the three neutral glycolipid fractions K0, K1, and K2 were heterogeneous. Therefore, signals of GL-11 appeared as minor signals among signals of GL-12 anomeric protons in the K2 spectrum (Figure 9, a, c, and d). Conversely, the K1 spectrum contained minor signals for GL-10 (Figure 9, arrow), in addition to GL-11 signals that were probably reinforced by GL-12 signals. The ^{1}H-NMR spectrum of K1 was interpreted by comparison with the spectra of K2 and SM1. The eight β-anomeric proton signals (Table 2), the resonance of IV-1 indicating a GlcNAcβ1→6 branch at β-Gal IV of a nLc$_6$ core, and the β-GlcNAc NAc signals at 1.826 and 1.846 ppm (III and V-V′, respectively) supporting the *iso*-nLc core structure were present. The intensity of the α-Gal H-1 signal was in agreement with two terminal Galα1→3 as in K2 (Figure 9). The presence of Fucα1→3 linked to →4GlcNAcβ1→ was indicated by the α-anomeric signal at 4.886 ppm (Figure 9, Table 3). A β-

Table 3. Diagnostic signals of Le^x-type Fucα1→3.

	H-1	*H-5*	*H-6*	*References*
III^{3}αFuc-nLc$_4$	4.876	4.590	1.020	31
VI^{3}NeuAcIII^{3}αFuc-nLc$_6$	4.878	4.589	1.014	16
X^{3}NeuAcVII^{3}αFuc-nLc^{10}	4.875	4.594	1.015	30
IV^{3}αGal III^{3}αFuc-nLc$_4$	4.889	4.578	1.031	15
VI^{3}NeuAcVI′^{3}αGal V′^{3}αFuc-*iso*-nLc$_8$	4.893	4.624	1.028	this work SM1
VI^{3}VI′^{3}(αGal)$_2$ V′^{3}αFuc-*Iso*-nLc$_8$	4.886	nd	1.045	this work K1

anomeric proton signal at 4.351 ppm, as in SM1, was assigned to the H-1 proton signal of a β-Gal VI′ in the vicinity of a Fucα1→3-substituted GlcNAc V′. The signal at 4.429 ppm (Figure 9, K1 spectrum, arrow) was interpreted as originating from the presence of GL-10 in the K1 fraction. The V′-1 signal of GL-11 was probably shifted downfield at 4.524 ppm (as indicated by the contaminant c signal in the K2 spectrum) and buried in high background together with the nearby Fucα1→3 H-5 quartet. This assignment was supported by the fact that the shape and intensity of the V-1/III-1 signals were identical in K1 and K2, ruling out fucosylation of GlcNAc III or GlcNAc V. Therefore, the major signals of the ^{1}H-NMR spectrum of K1 were consistent with the structure VI^{3}VI^3(αGal)$_2$V′^{3}αFuc-*iso*-nLc$_8$, in agreement with the major pseudomolecular ions of the MALDI-TOF mass spectrum (Figure 3, panel B), the reactivity with anti-Galα1→3Gal antibodies of native K1, and its reactivity with CD15 and 1B2, but not with anti-Le^a mAb, after α- galactosidase hydrolysis.

^{1}H NMR Signals for the structural components of ceramide

^{1}H NMR spectra of the olefinic region of the sialosylated glycolipids (Figure 8) displayed the characteristic pair of *trans*-vinyl proton signals of R4 (doublet of doublets at 5.37 ppm) and R5 (doublet of triplets at 5.55-5.56 ppm) (Table 4) of sphingenine (d18:1 sphingosine) [32]. Other signals for sphingosine were assignable in all spectra (R-6, R-3). The upfield spectra displayed the alkyl methyl resonance at 0.85 ppm (Figure 8) and the alkyl methylene resonance at 1.24 ppm. Resonances for FA in the sialosylated glycolipids were those of nonhydroxylated nFA-2 (2.04 ppm) with cis-allyl (1.98 ppm) and cis-vinyl (5.32 ppm) signals, indicating some degree of unsaturation (Figure 8, Table 4). Signals for nFA-2 and cis-allyl protons were interpretable in the K1 and K2 upfield spectra (Table 4), but signals for the cis-vinyl protons were buried by an impurity peak (Figure 9).

Discussion

Six high-molecular weight pig kidney cortex glycolipids were detected and separated on thin-layer chromatograms. They were characterized as deca-, undeca-, and dodecaglycosylceramides with a common *iso*-nLc core. These complex glycolipids were minor components, especially neutral glycolipids. Despite the very small amounts recovered by HPTLC purification, which prevented structural determinations by 2D ^{1}H NMR spectroscopy, they were successfully characterized by HPTLC associated with enzymatic degradation and immunostaining with antibodies, methylation analysis, and MALDI-TOF mass spectroscopy. In addition, 1D ^{1}H NMR spectroscopy was particularly useful because it was possible to rely on previously established spectra of *iso*-nLc core glycolipids [10, 16, 30], and because all glycolipids described herein, except K0, yielded reasonably good 400 MHz spectra, with three of them (K1, SM1, and SM2) being acquired for the first time. For interpreting the spectra, it was considered that the *iso*-nLc core consists of a nLc$_6$ chain with a branch attached to C6 of the fourth galactose, although during biosynthesis, addition of *N*-acetylglucosamine at C6 does not take place after completion of the nLc$_6$ chain but follows immediately the transfer of *N*-acetylglucosamine at C3 of galactose IV [33].

The structures described here were isolated from the kidney cortex of O-typed pigs, nonexpressing histo-blood group A, to avoid possible occurrence of A-active *iso*-nLc$_8$ dodecaglycosylceramide identical to A^c of human erythrocytes [34]. In the present study, neither H-active, nor H-active/sialosylated glycolipids as in human erythrocytes [35], were detected among complex glycolipids.

Complex Galα1→3Gal-terminated neutral glycolipids of pig kidney cortex have been first detected in our previous work characterizing GLe^x hexaglycosylceramide [15]. It was shown that the most polar Galα1→3Gal- reactive band on HPTLC actually contained GLe^x-expressing GL-12 and GL-11 (Table 1). In the present work, glycolipids were prepared from the kidney of 2-year-old pigs. The most polar Galα→3Gal-reactive neutral glycolipids were tentatively isolated by preparative HPTLC as three fractions, K0, K1, and K2, reactive with anti-Galα1→3Gal antibodies. Degalactosylated K0 and K1 were reactive with CD15, but not with anti-Le^a mAb, indicating the only presence of Le^x chains. The very low concentrations and overlapping ranges

Table 4. Resonances for Ceramide.

Signals for normal sphingosine (4-sphingenine)

	R-6	R-3	R-4	R-5	
VI^{3}NeuAc-*iso*-nlc$_8$	1.937	3.910	5.355	5.539	30
IV^{3}αGal-nLc$_4$	1.925	3.918	5.351	5.555	15
IV^{3}αGal III^{3}αFuc-nLc$_4$	1.944	3.928	5.357	5.555	15
VI^{3}VI′^{3}(NeuAc)$_2$-*iso*-nlc$_8$	1.941	3.914	5.372	5.555	this work SD1
VI^{3}NeuAcVI′^{3}αGal-*iso*-nLc$_8$	1.941	3.920	5.374	5.558	this work SM2
VI^{3}NeuAcVI′^{3}αGalV′^{3}αFuc-*iso*-nLc$_8$	1.943	3.921	5.377	5.567	this work SM1
VI^{3}VI′^{3}(αGal)$_2$-*iso*-nLc$_8$	1.944	3.918	5.374	5.557	this work K2
Vi^{3}VI′^{3}(αGal)$_2$ V′^{3}αFuc-*iso*-nLc$_8$	1.942	3.917	5.371	5.560	this work K1

Signals for non-hydroxylated FA with some degree of unsaturation

	nFA-2	cis-allyl	cis-vinyl	
VI^{3}NeuAc-*iso*-nLc$_8$	2.029	1.980	5.322	30
IV^{3}αGal-nLc$_4$	2.038	1.961	5.321	15
VI^{3}VI′^{3}(Neuac)$_2$-*iso*-nLc$_8$	2.038	1.979	5.324	this work SD1
VI^{3}NeuAcVI′^{3}αGal-*iso*-nLc$_8$	2.039	1.980	5.321	this work SM2
VI^{3}NeuAcVI′^{3}αGal V′^{3}αFuc-*iso*-nLc$_8$	2.041	1.981	5.321	this work SM1
VI^{3}VI′^{3}(αGal)$_2$-*iso*-nLc$_8$	2.038	1.982	n.d	this work K2
VI^{3}VI′^{3}(αGal)$_2$V′^{3}αFuc-*iso*-nLc$_8$	2.037	1.980	n.d	this work K1

of polarity generated by the fatty acid diversity prevented purification to homogeneity.

Characterization of the novel structures GL-11 (VI^{3}VI′^{3}(αGal)$_2$V′^{3}αFuc-*iso*-nLc$_8$Cer) and GL-12 (VI^{3}VI′^{3}(αGal)$_2$V^{3}V′^{3}αFuc-*iso*-nLc$_8$Cer) was performed with heterogeneous K0 and K1 fractions. The GL-11 structure was established by relying on an interpretable, although not of high quality, ^{1}H NMR spectrum of K1. The ^{1}H NMR unambiguously assigned the fucose residue to the 6-linked branch, and indicated that the sample was not a mixture of the two possible monofucosylated structures. The ^{1}H NMR spectrum obtained for K0 was not informative due to high background in the anomeric region. An additional element for the characterization of GL-12, compared with our previous work, was given by the MALDI-TOF mass spectrum of K1, which clearly indicated that GL-12 differed from GL-11 by addition of one fucose residue.

From our previous work, it is known that kidneys of young pigs express less GLe^x determinants than old animals [15]. Purification of kidney glycolipids from 3-month-old pigs allowed isolation of a homogeneous K2 fraction corresponding to GL-10 (Figures 2 and 3). However, the yield was not sufficient for ^{1}H NMR analysis. Therefore, ^{1}H NMR spectroscopy was performed with the K2 fraction isolated from the kidney of 2-year-old pigs. Thus, it contained small amounts of GL-11 (Figure 9). The present study indicated that K2/GL-10 was VI^{3}VI′^{3}(αGal)$_2$-*iso*-nLc$_8$Cer, which has been previously isolated from rabbit erythrocyte membranes and characterized by mass spectrometry and ^{1}H NMR spectroscopy [10].

It is likely that GL-11 and GL-12 are both synthesized from GL-10 by addition of one (GL-11) and two fucoses (GL-12) to C3 of the V-V′ *N*-acetylglucosamine residues. The relationship between the three structures was exemplified by the MALDI-TOF mass spectrum (Figure 3). This structural information reflects the probable pathway of GL-12 biosynthesis. According to the rule that the acceptor substrate of the α3-fucosyltransferase for synthesis of GLe^x

is the afucoB trisaccharide [36], a fucose is added first to the afucoB epitope of the 6-branch of GL-10, resulting in GL-11. Then, a second fucose is added to the 3-linked afucoB epitope to yield GL-12. This is the most probable pathway, although linkage of the second fucose to GlcNAc III cannot be ruled out in the absence of an informative ^{1}H NMR spectrum of K0. However, as K1 was a mixture of GL-11 and GL-12, linkage of Fucα1→3 to GlcNAc III would have induced additional typical downfield shifts for III-1 and IV-1 resonances (see GLe^x-6 in Table 2), which were not detected in the ^{1}H NMR spectrum of K1. The α3-fucosyltransferase of porcine kidney differs from the human transferase by its ability *in vivo* to transfer Fuc residues onto I-active core glycolipids. Branched Le^x or SLe^x have never been found in human tissues, although the human milk α3/4-fucosyl transferase has been used *in vitro* to synthesize oligosaccharides with multivalent sialosyl Le^x epitopes on both the 6-linked and 3-linked branches [37].

Two of the three sialosylated glycolipids, decaglycosylceramides SD1 and SM2, have already been described in other species. SD1 was identical to a disialosylated glycolipid characterized from human erythrocyte membranes [16]. SM2 was similar with an I-active glycolipid of bovine erythrocytes, first characterized on the basis of enzymatic degradation and methylation analysis [11]. This structure was recently confirmed by ^{1}H NMR analysis of the oligosaccharides released by ceramide glycanase hydrolysis, and *N*-glycolylneuraminic acid was found as major sialic acid [12]. In the present work, the ^{1}H NMR spectrum of the native glycolipid SM2 was obtained under standard conditions for glycolipids, in Me_2 SO-d_6/2%D_2O. Comparison with spectra of already described and new *iso*-nLc core glycolipids was thus possible. The ^{1}H NMR spectrum of SM2 unambiguously assigned NeuAcα(2→3) to the nLc_6 chain and α-galactose to the 6-linked branch. The presence of SM2 in porcine kidney was previously detected with HPTLC-immunostaining after neuraminidase hydrolysis, without structural characterization [38]. Based on the occurrence of VI^{3}NeuAcVI′^{3}αGal-*iso*-nLc_8Cer in porcine kidney, as in bovine erythrocytes, and of VI^{3}NeuAcVI′^{2}αFuc-*iso*-nLc_8Cer in human erythrocytes [35], it appears that, in hybrid structures, NeuAcα2→3 is always attached to the 3-linked branch of the *iso*-nLc_8 core. It is possible that an α2→3sialytransferase specific to the 3-linked branch of the *iso*-nLc_8 core is conserved among different species. Therefore, during the synthesis of disialosylated SD1 from *iso*-nLc_8Cer, linkage of NeuAc to the 6-linked branch probably occurs only after addition of NeuAc to terminal galactose of the nLc_6 chain (3-linked branch). Such a hypothesis is supported by the characterization of VI^{3}NeuAc-*iso*-nLc_8Cer, a glycolipid carrying a NeuAc α2→3-linked to the nLc_6 chain, with an unsubstituted 6-linked lactosamine [16, 30].

The ^{1}H NMR spectrum of SM1 was interpreted by comparison with spectra of SM2 and the previously characterized GLe^x-6 structure also isolated from porcine kidney cortex [15]. SM1 was found to be a novel structure, with a sialosylated 3-linked branch as other hybrid structures and a GLe^x determinant on the 6-linked branch, VI^{3}NeuAcVI,^{3}αGalIV,^{3}αFuc-*iso*-nLc_8Cer. The SLe^x determinant was undetectable among *iso*-nLc core, or nLc core glycolipids with 6 or 8 carbohydrate residues. This is in contrast with human kidney from which the SLe^x hexaglycosylceramide was originally isolated and characterized [39]. In agreement with the previous finding that the Le^x trisaccharide is not a substrate for the α3-galactosyltransferase [36], it can be concluded that Galα3-nLc is the preferential substrate of the α3-fucosyltransferase of porcine kidney, which appears unable to use *in vivo* NeuAcα3-nLc as acceptor. In the present study, absence of detectable unsubstituted Le^x glycolipids suggested that nLc is not a good substrate for porcine kidney α3-fucosyltransferase.

The present study confirmed the finding that the expression of the GLe^x epitope is developmentally regulated under the control of α3-fucosyltransferase [15]. Expression of VI^{3}NeuAcVI,^{3}αGa IV,^{3}αFuc-*iso*-nLc_8Cer (SM1) increased during the postnatal period and was maximum in older pigs, as already observed for GLe^x-6, -8, and -12 [15].

Acknowledgments

We thank Drs. J. LePendu (7-LE) and D. Blanchard (NaM87-1F6) for their generous gift of murine monoclonal antibodies. This work was supported by the Institut de la Santé et de la Recherche Médicale (INSERM), the Région des Pays dela Loire, and the Centre National de la Recherche Scientifique (CNRS) (Fellowship to J. L.).

References

1 Platt JL, Bach FH (1991) In *Xenotransplantation* (Cooper DKC, Kemp E, Reemtsma KI, White DJG, eds) pp 69–79. Berlin: Springer-Verlag.
2 Good H, Cooper DKC, Malcolm AJ, Ippolito RM, Koren E, Neethling FA, Ye Y, Zudhi N, Lamontagne LR (1992) *Transplantation Proc* 24: 559–62.
3 Galili U (1993) *Immunology Today* 14: 480–2.
4 Collins BH, Parker W, Platt JL (1994) *Xenotransplantation* 1: 36–46.
5 Galili U, Clark MR, Shohet SB, Buehler J, Macher BA (1987) *Proc Natl Acad Sci U S A* 84: 1369–73.
6 Galili U, Shohet SB, Kobrin E, Stults CLM, Macher BA (1988) *J Biol Chem* 263: 17755–62.
7 Galili U, Swanson K (1991) *Proc Natl Acad Sci U S A* 88: 7401–4.
8 Eto T, Ichikawa Y, Nishimura K, Ando S, Yamakawa T (1968) *J Biochem* (Tokyo) 64: 205–13.
9 Stellner K, Saito H, Hakomori (1973) *Arch Biochem Biophys* 155: 464–72.
10 Hanfland P, Egge H, Dabrowski U, Kuhn S, Roelcke D, Dabrowsky J (1981) *Biochemistry* 20: 5310–19.

11 Watanabe K, Hakomori S, Childs R, Feizi T (1979) *J Biol Chem* 254: 3221–8.
12 Dasgupta S, Hogan EL, Glushka J, van Halbeek H (1994) *Arch Biochem Biophys* 310: 373–84.
13 Jalali-Araghi K, Macher BA (1994) *Glycoconjugate J* 11: 266–71.
14 Samuelsson BE, Rydberg L, Breimer ME, Bäker A, Gustavsson M, Holgersson J, Karlsson E, Uyterwaal AC, Cairn T, Welsh K (1994) *Immunol Rev* 141:151– 68.
15 Bouhours D, Liaigre J, Naulet J, Maume D, Bouhours JF (1997) *Glycoconjugate J* 14: 29–38.
16 Levery SB, Nudelman ED, Kannagi R, Symington FW, Andersen FH, Clausen H, Baldwin M, Hakomori S (1998) *Carbohyd Res* 178: 121–44.
17 Bouhours D, Hansson GC, Angström J, Jovall PA, Bouhours JF (1992) *J Biol Chem* 267: 18533–40.
18 Saito T, Hakomori S (1971) *J Lipid Res* 12: 257–9.
19 Ueno K, Ando S, Yu RK (1978) *J Lipid Res* 19: 863–71.
20 Bouhours JF, Glickman RM (1976) *Biochim Biophys Acta* 441: 123–33.
21 Bouhours D, Bouhours JF, Dorier A (1982) *Biochim Biophys Acta*713: 280–84.
22 Bouhours D, Larson G, Bouhours JF, Lundblad A, Hansson GC (1987) *Glycoconjugate J* 4: 59–71.
23 Young WW, Portoukalian J, Hakomori S (1981) *J Biol Chem* 256: 10967–72.
24 Bouhours JF, Richard C, Ruvoen N, Barreau N, Naulet J, Bouhours D (1998) *Glycoconjugate J* 15: 93–9.
25 Ciucanu I, Kerek F (1984) *Carbohydr Res* 131: 209–17.
26 Yang H, Hakomori S (1971) *J Biol Chem* 246: 1192–200.
27 Oriol R, Ye Y, Koren E, Cooper DKC (1993) *Transplantation* 56:1433–42.
28 Holgersson J, Joval PA, Samuelsson BE, Breimer ME (1990) *J Biochem (Tokyo)* 108: 766–77.
29 Watanabe K, Laine RA, Hakomori S (1975) *Biochemistry* 14: 2725–33.
30 Stroud MR, Handa K, Salyan MEK, Ito K, Levery SB, Hakomori S, Reinhold BB, and Reinhold VN (1996) *Biochemistry* 35: 758–69.
31 Levery SB, Nudelman ED, Andersen NH, Hakomori S (1986) *Carbohyd Res* 151: 311–28.
32 Koerner TA, Prestegard JH, Demou PC, Yu RK (1983) *Biochemistry* 22: 2676– 87.
33 Piller FP, Cartron JP, Maranduba A, Veyrières A, Leroy Y, Fournet B (1984) *J Biol Chem* 259: 13385–90.
34 Fukuda MN, Hakomori S (1982) *J Biol Chem* 257: 446–55.
35 Watanabe K, Powell M, Hakomori S (1978) *J Biol Chem* 253: 8962–67.
36 Joziasse DH, Schiphorst WE, Koeleman CA, Van den Eijnden DH (1993) *Biochem Biophys Res Commun* 194: 358–67.
37 Renkonen O, Toppila S, Penttilä L, Salminen H, Helin J, Maaheimo H, Costello CE, Pekka Turunen J, Renkonen R (1997) *Glycobiology* 7: 453–61.
38 Hendricks SP, He P, Stults CL, Macher BA (1990) *J Biol Chem* 265: 17621–6.
39 Rauvala H (1976) *J Biol Chem* 251: 7517–20.

Received 14 January 1998, revised 23 April 1998, accepted 22 May 1998